Supplementary Materials

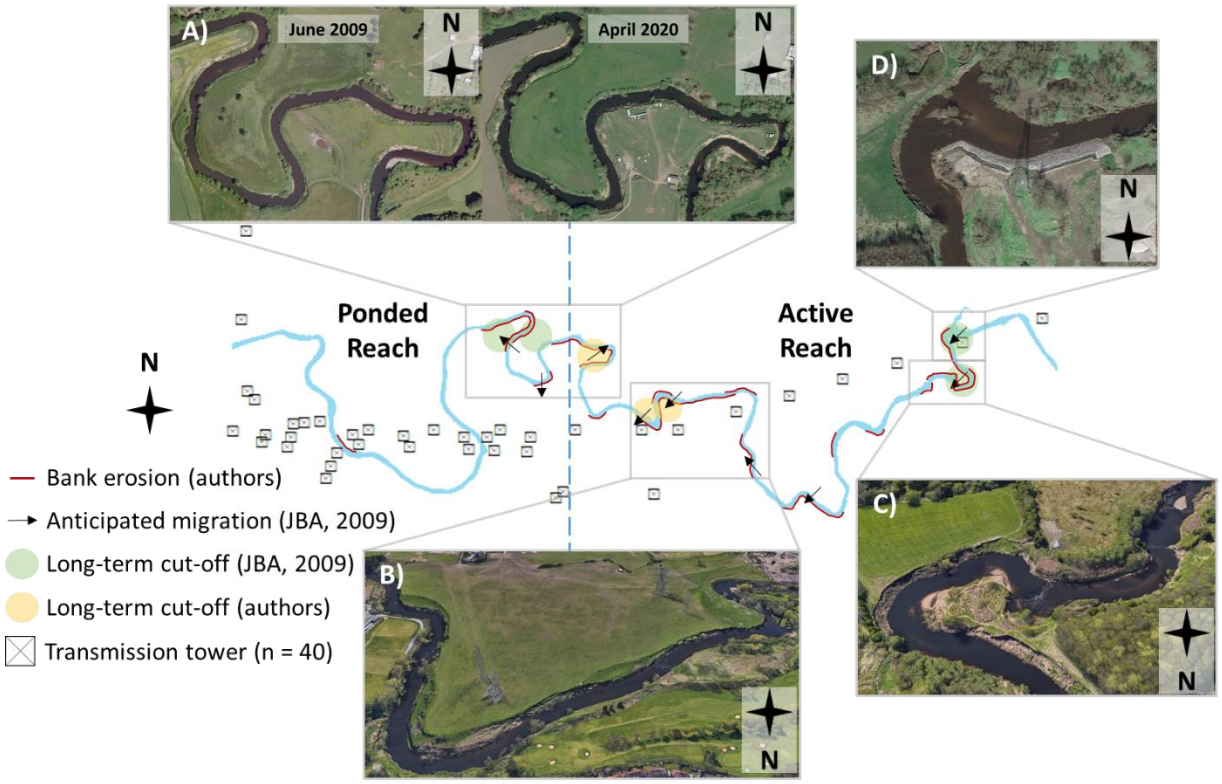

Figure S1: A model of system function for the River Mersey reach (adapted from one originally produced by JBA (2009) and updated by this paper's authors to reflect changes that have occurred over the past 10 years based on aerial images © Google Earth). The valley is split into an 'active reach' upstream, characterised by extensive contemporary erosion along much of the riverbanks, significant long-term lateral migration with a high likelihood of meander bend cut-offs forming in several places (based on JBA's study and our assessment of aerial imagery), and high susceptibility to overbank flooding; and a 'ponded reach' downstream, also prone to overbank flooding but with more subdued rates of lateral migration, fewer locations likely to experience meander bend cut-offs, and more minor and localised contemporary erosion. A selection of aerial images is displayed to give the reader some additional perspective of contemporary conditions along the channel. These images show: A) the evolution of some meander bends between Flixton and Carrington from June 2009 to April 2020; B) extensive bank erosion south of Flixton, potentially placing several National Grid transmission towers at risk of being undermined by the moving river channel; C) a closer look at rotational slump failure along several metres of riverbank along both sides of the channel near Urmston; and D) imagery from March 2017 showing protection measures (installed in 2015) along the southern riverbank to attempt to forestall bank erosion near tower, ZZN014 near Urmston. Transmission tower points © National Grid UK. Note the compass direction in each panel.

Text S1: Summary of recent protection measures installed at towers ZZN018 and ZZN024.

Works were carried out during route refurbishments in 2013-2014 at tower ZZN018. These works comprised bank reinforcement and channel reinstatement works costing in the order of £0.15 m. Just to the northwest, along the bank that ZZN018 sits atop, rock armour was placed along a 100-metre length of the river bank and at the base of the tower cofferdam to prevent further erosion. Rock armour, consisting of ~6000 tonnes of ~600 mm rocks, was placed 60 metres upstream and 40 metres downstream of the tower. This 'building out' into the river channel was agreed with the Environment Agency and involved some re-grading of the channel bed. Vegetation was also to be planted on the higher sections of riverbank to enhance the stability of the soil. Vegetation colonisation of the riverbank and the rock armour structure (installed in 2015) can be observed in freely available historical aerial imagery on Google Earth from March 2017 to April 2018 and images available thereafter.

The rationale for the rock armour installation came about as the original strategy, which called for an 'armorflex' (a flexible, interlocking matrix of concrete blocks of uniform size and weight used to control erosion caused by wave action) solution, was no longer suitable due to requirements for extensive re-grading of the riverbank slopes and the need to remove many tonnes of soil (which were also laced with Japanese Knotweed and Himalayan Balsam) from site. The removal of this soil thus becomes very costly and risky due to the controls placed, by law, on handling invasive species. Therefore, a solution was required which minimised contact with invasive vegetation as far as reasonably practicable, leading to installation of rock armour as the new choice of protection.

There is evidence near ZZN018's location of older tower structure foundations in the river channel. While, information on this is unavailable, it is likely to indicate previous relocation works of tower, ZZN018 mentioned in da Luz et al. (2015). Similar relocation works today may exceed £0.2 m in cost.

There is also evidence of attempts to protect the bank at tower ZZN024. These works near ZZN024 were not undertaken by National Grid and we believe consist of little more than tipping building spoil over the bank side.

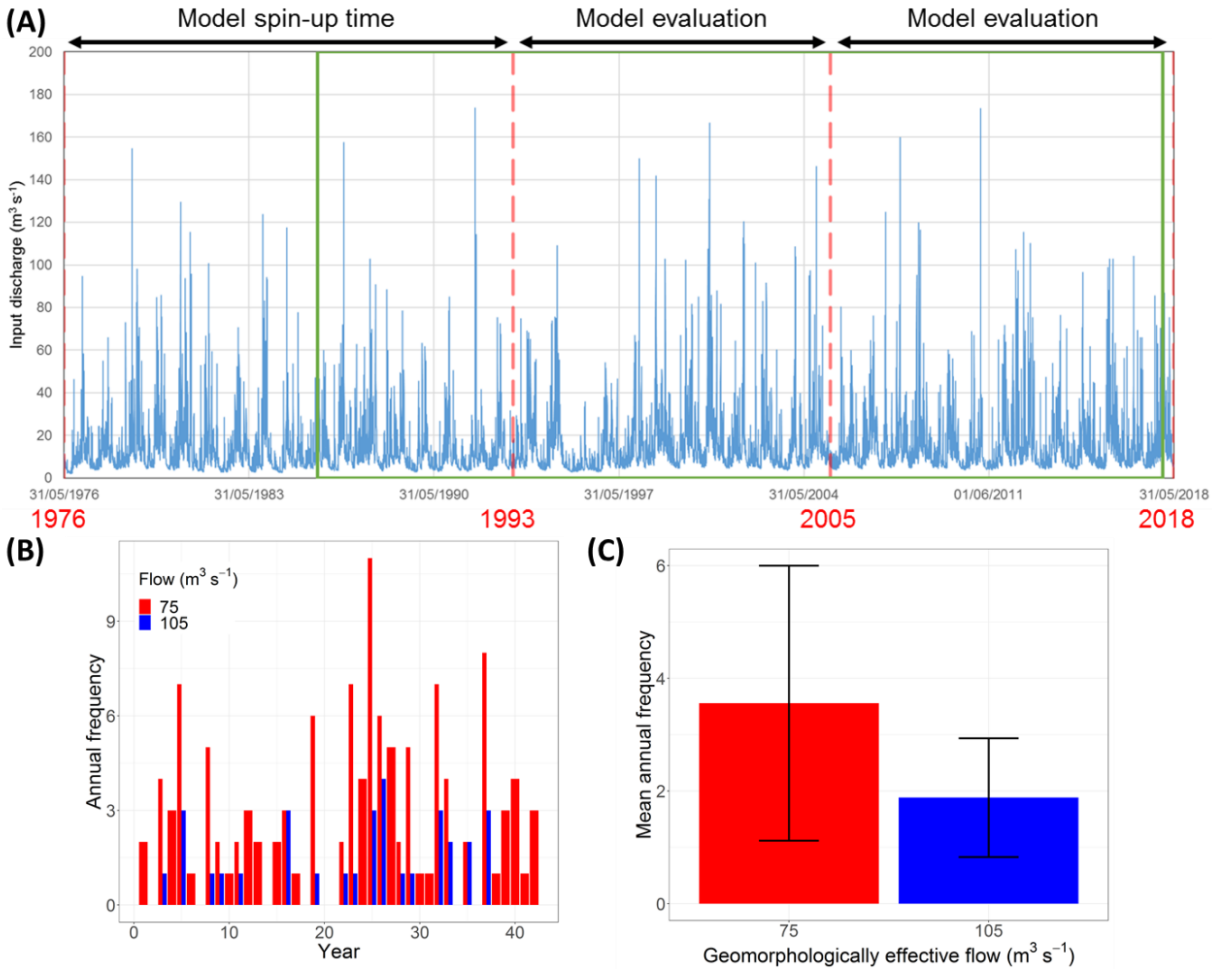

Figure S2: (A) Historic time-series (31/05/1976-31/05/2018) of daily stream flows from Ashton Weir at the reach inlet (NRFA, 2020). Years in red mark the dates of available Ordnance Survey maps. The green box marks the latter 32-year time-series used to create the six hydro-climate scenarios. (B) Time-series of the annual frequency of geomorphologically effective flows (75-105 m^3 s^{-1}). (C) The mean annual frequency of the geomorphologically effective flows (±1 standard deviation). Geomorphologically effective flows of parts (A) and (B) are summarised for the entire 42-year record, not the 32 years used to drive simulations.

Table S1: CAESAR-Lisflood parameters used to model channel changes along the Mersey.

Parameter (unitless unless stated otherwise)	Value(s) chosen			
Sediment				
Grain size and relative proportions	*Size (m)*	*Floodplain*	*Channel*	*Default*
	0.000002	0.3	0	0.144
	0.00006	0.35	0	0.022
	0.002	0.2	0.05	0.019
	0.004	0.1	0.1	0.029
	0.008	0	0.15	0.068
	0.016	0	0.25	0.146
	0.032	0.05	0.3	0.220
	0.064	0	0.1	0.231
	0.128	0	0.05	0.121
Suspended fraction | Fall velocity (m s^{-1})	Yes | 5.4×10^{-7}			
Transport equation	Wilcock & Crowe (2003) transport model			
Max velocity to calculate shear stress (m s^{-1})	5			
Max erode limit (m)	0.01			
Active layer thickness (m)	0.3			
Proportion of output sediment recirculated	1			
In-channel erosion rate λ*	Experimented values between 10 & 20			
Lateral erosion rate θ ($\times 10^{-5}$)*	Experimented values between 1 & 10			
No. of passes for edge smoothing filter	50			
No. of cells to shift erosion downstream	5			
Max difference for cross-channel smoothing^	0.0001			
Slope processes (*all other parameters in here are unused or left as default values*)				
Slope failure threshold (degrees)	50 (maximum slope identified from DEM)			
Vegetation				
Vegetation critical shear strength (N m^{-2}) ±	80			
Grass maturity (years)#	1			
Proportion of erosion allowed at maturity+	0.2			
Flow model (*discharge units = m^3 s^{-1}*)				
Input/output discharge difference allowed	9			
Min | max discharge for depth calculation	0.15 | 1000			
Water depth to exceed before erosion (m)	0.01			
Slope for edge cells (m m^{-1})	0.0001			
Evaporation rate (m day^{-1})	0.00025			
Courant number	0.3			
h_{flow} threshold (m)	0.00001			
Froude number (flow limit)	0.8			
Manning's *n* hydraulic roughness value	0.04 (look-up table in Chow, 1959)			

*The parameters which are changed one-at-a-time to calibrate the model.

^This controls lateral redistribution of sediment from the outer to the inner channel bank.

±Vegetation critical shear strength based on values from Fischenich (2001).

#Grass assumed to fully mature within a year (Lack & Evans, 2001).

+Proportion of erosion at maturity is set assuming grass allows twice as much erosion as forest (which we assume to be a minimum of 0.1) and based on a relationship between plant biomass and geomorphic work (Trimble, 2004).

Text S2: The lateral erosion and in-channel erosion parameters within CAESAR-Lisflood.

Two parameters governing river channel erosion required calibration: the lateral erosion rate parameter θ, and the in-channel erosion rate parameter λ. These are as follows:

$$E_{lat} = \frac{1}{R_{ca}} \theta \tau T \qquad (1)$$

where E_{lat} is the rate of lowering of riverbank cell elevations [m time-step^{-1}], R_{ca} is the radius of bend curvature [m], θ is a user-specified lateral erosion parameter [-], τ is the flow shear stress exerted by an inundated cell next to the channel bank [N m^{-2}] and T is time [s];

$$\Delta Z_{n-1} = V_{n-1} \lambda \frac{(Z_n - Z_{n-1})}{D_x} \qquad (2)$$

where ΔZ is the change in cell elevation [m] between time iterations, V is the volume of eroded sediment [m^3], D_x is the grid cell size [m], λ is the user-specified in-channel erosion rate [-], and n and $n - 1$ refer to the donor and recipient cells in the context of sediment routing between cells, respectively.

Equation (1) governs how rapidly the channel migrates laterally. Channel edge cells are identified using an edge-smoothing filter in the model during simulation (Coulthard & Van De Wiel, 2006). Repeated passes of this edge-smoothing filter calculate whether the channel edge cells reside along the inside or the outside of a meander bend based on the number of adjacent wet and dry cells. This calculation provides an estimate of the local radius of curvature R_{ca}, for each grid cell (Coulthard et al., 2007). These R_{ca} estimates are input into Equation (1), along with the user-specified θ parameter and local flow shear stresses to calculate the lateral erosion rate. The accuracy of R_{ca} depends upon parameterisation of the edge-smoothing filter and the number of cells to shift lateral erosion downstream, and these were set based on the average meander wavelength in the reach (following Van De Wiel et al., 2007).

Equation (2) controls the hydraulic radius of the channel and allows sediment to move laterally across the channel width independent to the effects of planform sinuosity resulting from Equation (1) (Coulthard et al., 2013). The value of λ governs how much sediment is transferred between cells n and $n - 1$ (higher values result in greater volumes of inter-cell sediment transfer). Adjusting values of λ in effect adjusts the cohesive strength of the floodplain sediments with lower values restricting channel widths, but enhancing depth, implying a greater degree of sediment cohesion (Coulthard et al., 2013).

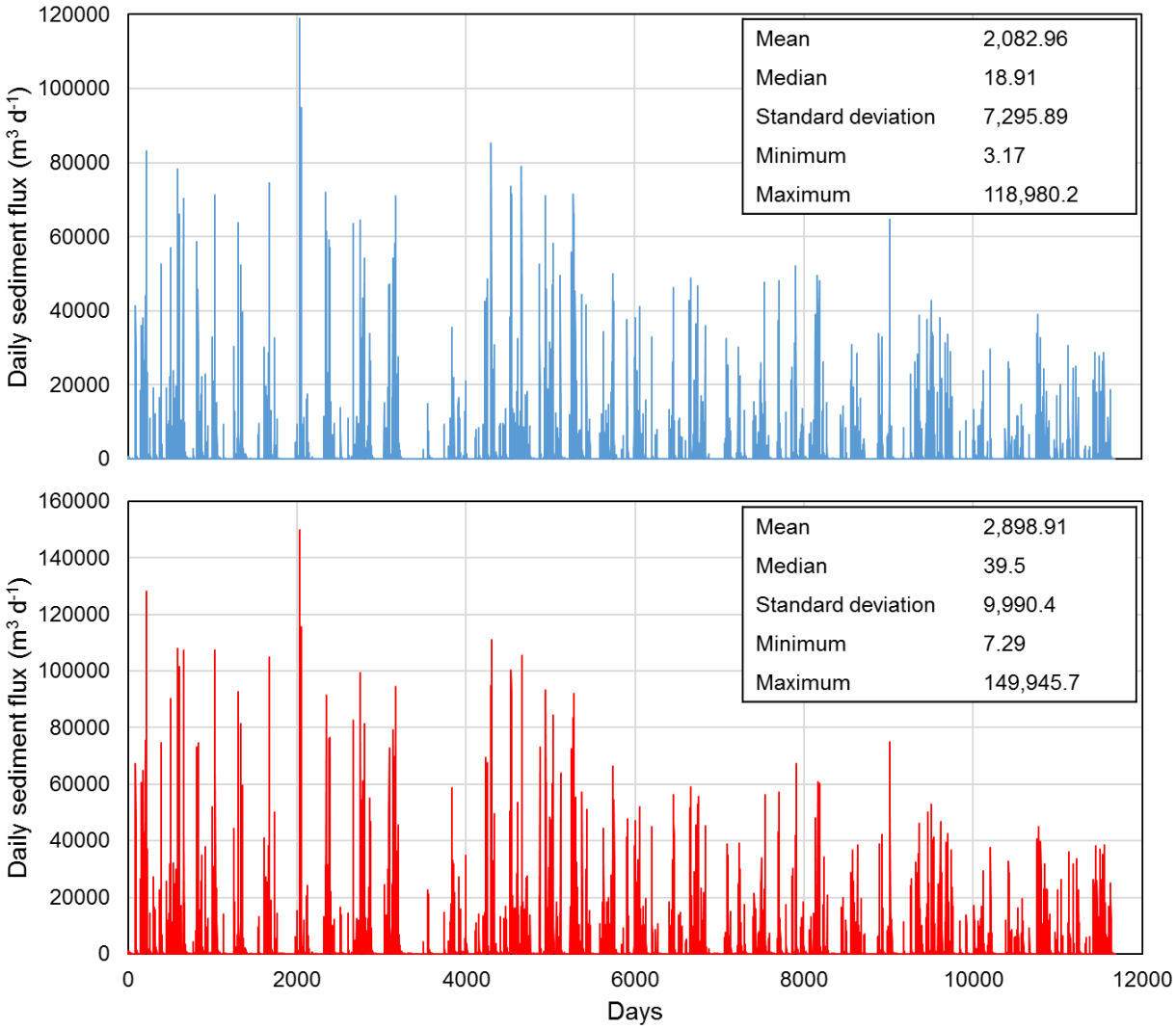

Figure S3: Daily sediment fluxes incorporated into the hydro-climate scenarios input into the Low (blue) and High (red) models. During model calibration, only a stream flow time-series is fed into the reach. As flows work their way through to the channel outlet, sediment is entrained and recorded at the outlet as daily sediment flux. In CAESAR-Lisflood, generated sediment fluxes can be recirculated so that fluxes recorded at the outlet on day, *n* are fed into the reach inlet on day, *n+1*. As geomorphic changes and resulting sediment flux differs between the Low and High models, each has a separate 32-year time-series of daily sediment fluxes that is incorporated with the flow series.

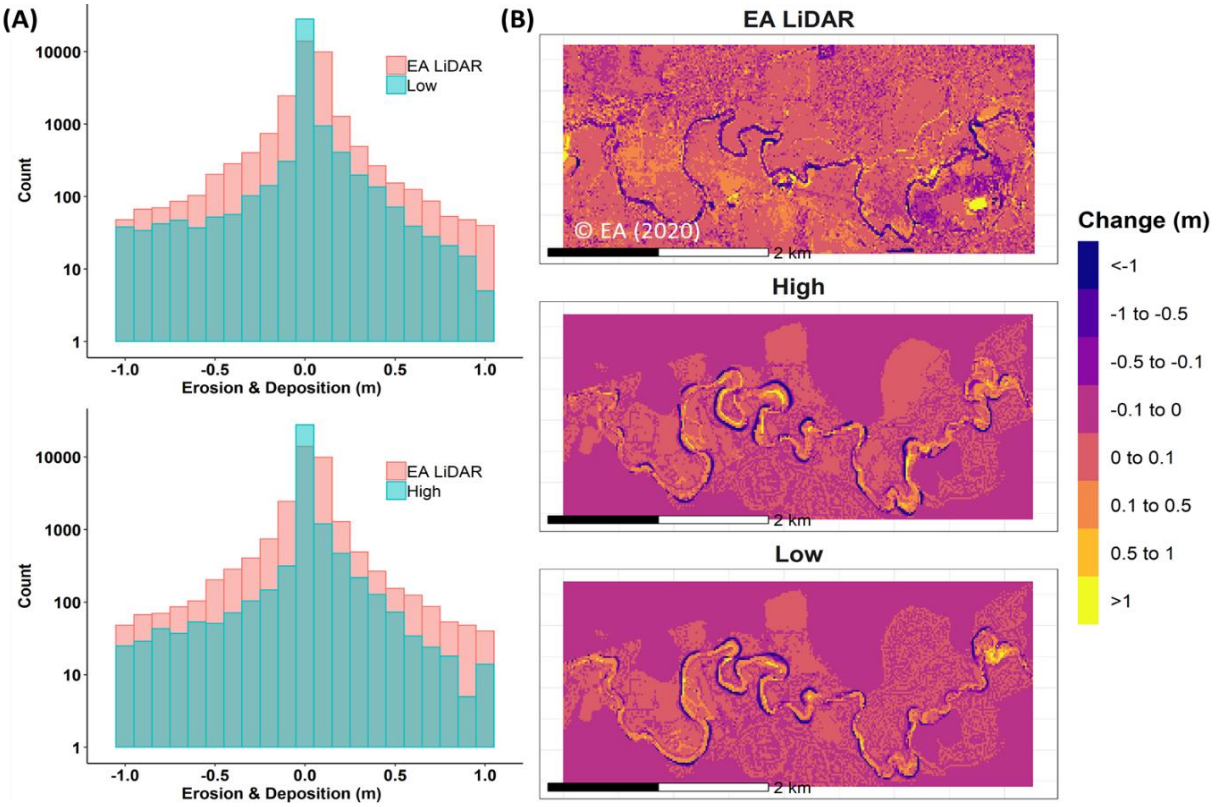

Figure S4: (A) Histograms comparing erosion (negative values) and deposition (positive values) from 2006 to 2018/19 between EA LiDAR data and the 2 models; (B) DEMs of Difference showing the spatial distribution of various depths of erosion (purple shades) and deposition (orange shades).

Figure S5: Locations and names of all forty electricity transmission towers (© National Grid UK) in the modelled reach.

Supplementary Materials References

Chow, V. T. (1959). *Open Channel Hydraulics*. McGraw-Hill: New York.

Coulthard, T. J., Hicks, D. M., & Van De Wiel, M. J. (2007). Cellular modelling of river catchments and reaches: Advantages, limitations and prospects. *Geomorphology*, *90*(3–4), 192–207. https://doi.org/10.1016/j.geomorph.2006.10.030

Coulthard, T. J., Neal, J. C., Bates, P. D., Ramirez, J., de Almeida, G. A. M., & Hancock, G. R. (2013). Integrating the LISFLOOD-FP 2D hydrodynamic model with the CAESAR model: implications for modelling landscape evolution. *Earth Surface Processes and Landforms*, *38*(15), 1897–1906. https://doi.org/10.1002/esp.3478

Coulthard, T. J., & Van De Wiel, M. J. (2006). A cellular model of river meandering. *Earth Surface Processes and Landforms*, *31*(1), 123–132. https://doi.org/10.1002/esp.1315

da Luz, R. A., Lawson, N., Douglas, I., & Rodrigues, C. (2015). Historical sources and meandering river systems in urban sites: the case of Manchester, UK. *North West Geography*, *15*(2), 1–27. https://doi.org/10.2307/j.ctv6gqvxj.120

Feeney, C. J., Chiverrell, R. C., Smith, H. G., Hooke, J. M., & Cooper, J. R. (2020). Modelling the decadal dynamics of reach-scale river channel evolution and floodplain turnover in CAESAR-Lisflood. *Earth Surface Processes and Landforms*, *45*(5), 1273-1291 https://doi.org/10.1002/esp.4804

Fischenich, C. (2001). *Stability Thresholds for Stream Restoration*. Engineer Research and Development Center: Vicksburg, MS.

JBA (2009). Assessment of fluvial erosion risk to pylons at Partington on the River Mersey, *Final Report 22nd December 2009*, JBA consulting.

Lack A. J., Evans D. E. (2001). *Plant Biology*. Springer-Verlag: New York

NRFA (2020). '69007 - Mersey at Ashton Weir', https://nrfa.ceh.ac.uk/data/station/info/69007 (accessed 04/03/21).

Trimble, S. (2004). Effects of riparian vegetation on stream channel stability and sediment budgets. In *Riparian Vegetation and Fluvial Geomorphology – Water Science and Application*, Bennett, S. J., Simon, A. (eds). American Geophysical Union: Washington, D.C.; 153–169.

Van De Wiel, M. J., Coulthard, T. J., Macklin, M. G., & Lewin, J. (2007). Embedding reach-scale fluvial dynamics within the CAESAR cellular automaton landscape evolution model. *Geomorphology*, *90*(3–4), 283–301. https://doi.org/10.1016/j.geomorph.2006.10.024

Wilcock, P. R., & Crowe, J. C. (2003). Surface-based transport model for mixed-size sediment. *Journal of Hydraulic Engineering*, *129*(2), 120–128.